molecular pharmaceutics

Article

pubs.acs.org/molecularpharmaceutics

Near Infrared Imaging of Indocyanine Green Distribution in Pregnant Mice and Effects of Concomitant Medications

Ameer Bishara,[†] Michal Meir,[†] Emma Portnoy, Miri Shmuel, and Sara Eyal*

Institute for Drug Research, School of Pharmacy, The Hebrew University of Jerusalem, Jerusalem, Israel

Supporting Information

ABSTRACT: The transfer of indocyanine green (ICG) across the placenta is considered to be very low based on measurements in fetal blood. The goal of this study was to evaluate in mice ICG's distribution within fetuses themselves and effects of concomitant medications on fetal exposure. Mid-gestational (day 12.5) and late-gestational (day 17.5) age mice were imaged after administration of ICG (0.167 mg), in the presence and the absence of the organic anion transporting polypeptide (OATP) inhibitor rifampin (10 mg/kg, n = 11, or 20 mg/kg, n = 1) or the P-glycoprotein inhibitor valspodar (12.5 mg/kg). In vivo ICG emission intensity was followed by ex vivo analysis of blood and tissue emission. Both valspodar and rifampin increased ICG's emission intensity within maternal tissues. In addition, valspodar enhanced the ex vivo signal in mid-pregnancy placentae (2.1-fold; $p < 0.01$) and fetuses (2.4-fold; $p < 0.01$), and reduced late-pregnancy placenta:blood and fetus:blood ratios. Rifampin increased placental (1.4-fold, $p < 0.05$, and 2.3-fold, $p < 0.01$, in mid- and late-pregnancy, respectively) and fetal (2.2-fold, $p < 0.01$, and 3.2-fold, $p < 0.01$, in mid- and late-pregnancy) ICG signal. Similarly to valspodar, late-pregnancy placenta:blood and fetus:blood ratios were reduced by rifampin. Both inhibitors enhanced ICG's emission in fetal leg, liver, and brain. In conclusion, ICG distribution into the mouse fetus can be enhanced when used concomitantly with OATP or P-glycoprotein inhibitors. The greater distribution within individual fetal tissues is likely related to ICG's greater transplacental transfer. Until further data are available on ICG's safety when combined with medications that affect its maternal handling, such combinations should be used with caution.

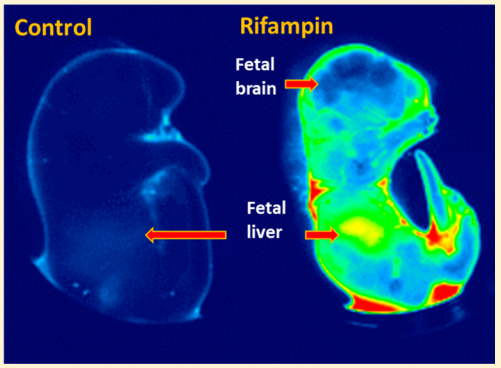

KEYWORDS: *molecular imaging, near-infrared imaging, indocyanine green, pregnancy, placenta, P-glycoprotein, organic anion transporting polypeptides*

INTRODUCTION

Indocyanine green (ICG), a tricarbocyanine dye, is the only United States Food and Drug Administration (FDA) and European Medicines Agency approved near-infrared probe. ICG has been used for decades for evaluation of hepatic function[1] and for ophthalmic angiography,[2] based on its lack of toxicity at the doses employed and its unique pharmacokinetics. ICG is highly bound to plasma proteins[3−6] and distributes uniformly in the blood within 2 to 3 min after intravenous injection.[4] It is exclusively cleared unchanged by the liver,[4] and hepatic clearance is limited by blood flow.[7] Uptake into hepatocytes is mediated by the organic anion transporting polypeptide (OATP) 1B3 and the human Na^+-taurocholate cotransporting polypeptide,[8] and excretion into the bile is mostly through the multidrug resistance proteins MDR3 and MRP2.[9] More recently, we have shown that P-glycoprotein (P-gp) also contributes to ICG's efflux from cells.[10] In addition to its use as the free compound, ICG has also been encapsulated into various nanostructures that alter its kinetics and utilized in experimental animal models for imaging tissues and body fluids.[11−13]

ICG has been given to pregnant women without adverse effects in the mother or the fetus, and studies since the 1960s demonstrated that ICG does not cross the placenta.[2,14−18] However, as with other compounds given to pregnant women, the FDA-approved label of ICG preparations states that "it is ... not known whether [ICG] can cause fetal harm when administered to a pregnant woman or can affect reproduction capacity. [ICG] should be given to a pregnant woman only if clearly indicated."[19]

The distribution of ICG within the fetus and the outcomes of concomitant use of modulators of transporter function in terms of fetal exposure to ICG have not been studied. Our aim was to evaluate ICG's fetal distribution and the effect of rifampin, an OATP inhibitor, and valspodar, a P-gp inhibitor, on ICG kinetics in pregnant mice.

EXPERIMENTAL SECTION

Materials. ICG was purchased from Acros Organics (Geel, Belgium). Valspodar (PSC-833) was from Tocris Bioscience (Bristol, U.K.). Pentobarbital sodium (Pental) was from CTS

Received: May 15, 2015
Revised: June 20, 2015
Accepted: July 6, 2015
Published: July 6, 2015

DOI: 10.1021/acs.molpharmaceut.5b00374
Mol. Pharmaceutics 2015, 12, 3351−3357

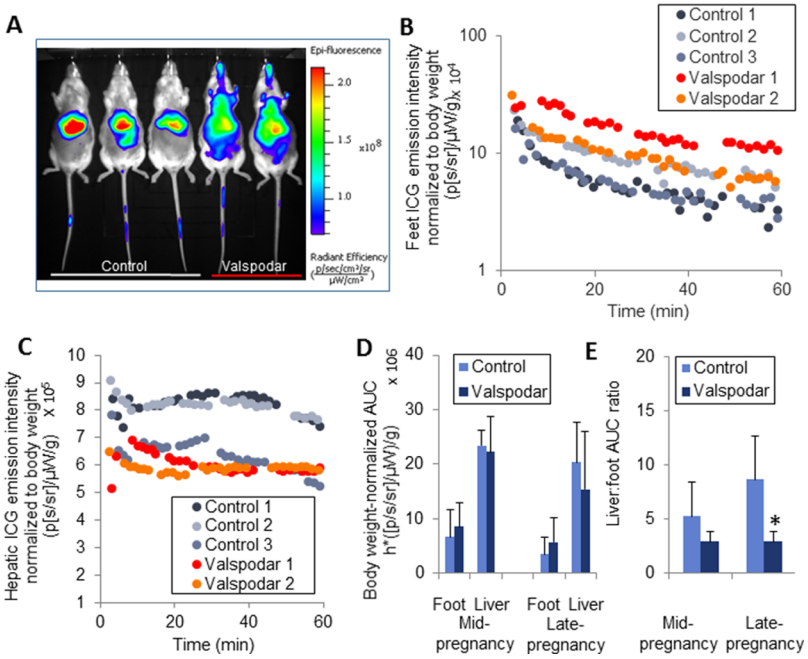

Figure 1. Valspodar alters maternal ICG kinetics in vivo. Mice in mid- or late-pregnancy were treated with 12.5 mg/kg valspodar or the vehicle. Shown are images from a representative study of mice in mid-pregnancy treated with 12.5 mg/kg valspodar or the vehicle and 0.167 mg of ICG (A), representative concentration−time profiles (same experiment) of ICG emission intensity in the presence or the absence of valspodar in the feet (B) and the liver (C), $AUC_{0-30min}$ values of ICG emission intensity (D), and the liver:foot emission intensity ratios (E) across all animals. Emission intensity here and in subsequent figures is shown as fold difference compared to the intensity of vehicle-treated mice at the same gestational age. The time from ICG injection to image acquisition in panel A was 11.6, 12.6, and 14.6 min for controls and 6.6 and 8.6 min for valspodar-treated mice. Data are shown as mean ± SD. The numbers of animals were 8 and 7 for control and valspodar-treated groups at mid-pregnancy and 5 and 6 for control and valspodar groups at late-pregnancy, respectively. *$p < 0.05$, significantly different from vehicle-treated mice of the same gestational age, Mann−Whitney test.

(Kiryat Malachi, Israel). Heparin sodium was from Rotexmedica (Trittau, Germany). All the other reagents were purchased from Sigma-Aldrich (Rehovot, Israel).

Animals. The experimental studies and protocols were approved by the Animal Care and Use Committee of the Hebrew University, protocol #13051, and the procedures followed were in accordance with the institutional guidelines. Pregnant female wild type FVB mice (8−10 weeks old) were purchased from Harlan Laboratories (Rehovot, Israel) and housed in the specific pathogen-free facility (SPF) unit at the Ein Kerem campus of the Hebrew University. The mice, initially weighing 15 to 30 g (depending on the gestational age), had free access to food (a standard diet) and water and were maintained on a 12:12 h automatically timed light/dark cycle. Studies were conducted on gestational days 12.5 or 17.5, representing mid- and late-gestation, respectively (term in mice is 20−21 days).

In Vivo Imaging Studies. The valspodar and the rifampin studies were separated from one another because the maximal capacity of the in vivo imaging system (IVIS) is five animals and we aimed at including at least two controls (not treated with transporter inhibitors) on each study day. Under isoflurane (1−2%, v/v) anesthesia, mice were shaved and underwent a baseline scan by IVIS Kinetic (Caliper Life Sciences, Hopkinton, MA, USA). Valspodar (12.5 mg/kg, $n = 9$ for mid-pregnancy and $n = 6$ for late pregnancy; near-minimal dose applied in mice to inhibit blood−brain barrier P-gp[20]) or rifampin (10 mg/kg, $n = 8$ for mid-pregnancy, and $n = 3$ and $n = 1$ for late pregnancy, at 10 and 20 mg/kg respectively; initial dose based on van de Steeg et al., 2010,[21] and later lowered to avoid toxicity); both substances in polyethylene glycol 300:ethanol 80:20; or the vehicle ($n = 8$ and $n = 6$ for the mid- and late-pregnancy valspodar studies, and $n = 6$ and $n = 4$ for the rifampin studies, respectively) was administered intraperitoneally (maximal volume 200 μL/mouse). 45 min later, ICG (0.167 mg; injected concentration 1 mM, in a solution consisting of 10 parts double distilled water and 2 parts filtered 2 mM phosphate buffer containing 9.3% sucrose) was injected into the tail vein in a total volume of 200 μL. The dose was selected based on our previous experience with ICG studies in mice,[10] to allow detection and quantification of ICG emission in the fetus. Mice were repetitively scanned over a time period of 30−60 min, while body temperature was kept on a 37 °C platform (excitation wavelength 745 nm, emission 840 nm).

At the completion of the in vivo scans, mice were sacrificed under pentobarbital sodium anesthesia (200 mg/mL, 350 mg/kg) and maternal cardiac blood samples (40 μL) were collected in heparinized 96-well plates. Subsequently, fetuses and placentae, followed by maternal liver and kidneys, were collected. Along the collection procedure, tissue and blood samples were protected from light and kept on ice. Immediately after that, they were scanned by a Typhoon FLA 9500 biomolecular imager (GE Healthcare Life Sciences, Piscataway Township, NJ, USA; excitation wavelength 785 nm, emission 820 nm).

Image Analysis. For analysis of the in vivo ICG kinetics, regions of interest (ROIs) were drawn over maternal livers (0.35 cm^2) and feet (0.07 cm^2) using Living Image 4.3.1 (PerkinElmer, Waltham, MA, USA). The feet were selected as the reference background region because they are remote from the injection site, the placenta and the liver (the latter shown in

DOI: 10.1021/acs.molpharmaceut.5b00374
Mol. Pharmaceutics 2015, 12, 3351−3357

preliminary studies to exhibit high ICG emission), can be clearly identified, and do not contain tissues known to highly express P-gp or OATPs.[22] The emission intensity of each sample was expressed in radiant efficiency units ([photons/second/steradian]/microwatt; [p/s/sr]/μW). ICG area under the concentration−time curve (AUC) was calculated using WinNonlin 6.2 (Pharsight, MountainView, CA). The AUC values were normalized to maternal body weight and were calculated over the first 30 min after ICG injection ($AUC_{0-30min}$), which was the minimal scan time common to all animals.

The ex vivo emission intensity was analyzed using ImageJ 1.47 V (National Institutes of Health, Bethesda, Maryland, USA). For presentation purposes, images of fetuses were analyzed by PMOD 3.3 (PMOD Technologies Ltd., Zurich, Switzerland). All emission intensity values were normalized to maternal weight. Because of the between-day variability in the values of ex vivo emission intensity, data of each experiment were normalized to the mean of controls of the same study day. Fetal values were normalized to the mean of fetal legs in control animals of the same study day. In addition, optical imaging is confounded by variation in the extent of light attenuation in different organs and tissues.[23] Therefore, the estimation of treatment effects (fold-change) was quantitative, whereas comparisons between tissues were semiquantitative only. Values are shown as organ emission intensity (arbitrary units; a.u.) and organ/blood or fetal organ/leg ratios.

Statistical Analysis. Data are reported as means ± SD. Emission intensity and AUC values were compared using the nonparametric Mann−Whitney test (two-tailed test) (InStat; GraphPad, La Jolla, CA, USA). P value ≤0.05 was considered significant.

RESULTS

Following intravenous administration, ICG's peripheral emission intensity appeared to be greater and the hepatic signal appeared to be lesser in valspodar-treated mice than in controls (Figure 1A−C). These changes were not statistically significant (Figure 1D). However, when normalized to the foot emission intensity, the hepatic fluorescence of mice treated with valspodar was 3-fold ($p < 0.05$) lesser than that of controls in late-gestation (Figure 1E). Ex vivo, valspodar tended to increase the emission intensity in maternal tissues, although high between-mice variability impaired the analysis of the treatment effect. The changes were significant for maternal blood in late-pregnancy and the kidneys in mid-pregnancy (Figure 2A). In addition, valspodar enhanced the emission intensity of ICG in mid-pregnancy placentae (2.1-fold; $p < 0.01$) and fetuses (2.4-fold; $p < 0.01$), and reduced the late-pregnancy placenta:blood and fetus:blood ratios (Figure 2B).

Similarly to valspodar, rifampin did not significantly alter the systemic or hepatic ICG distribution in vivo (Figure 3A). Likewise, rifampin did not affect the liver:foot $AUC_{0-30min}$ ratios (Figure 3B). However, ex vivo analysis revealed significant increases in the ICG signal in maternal liver (late-pregnancy; $p < 0.05$) and kidneys (both gestational ages; $p < 0.05$; Figure 3B). In addition, rifampin enhanced the placental and fetal ICG signal at both gestational ages (1.4-fold, $p < 0.05$, and 2.3-fold, $p < 0.01$, in mid- and late-pregnancy placentae, and 2.2-fold, $p < 0.01$, and 3.2-fold, $p < 0.01$, in mid- and late-pregnancy fetuses, respectively). Normalization to the blood intensity demonstrated an opposite trend in late pregnancy, with reduced placenta:blood and fetus:blood ratios following

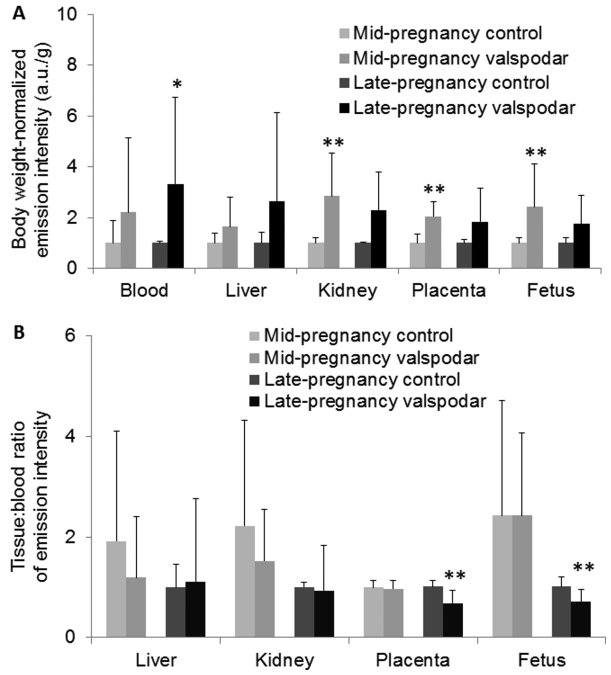

Figure 2. Ex vivo analysis of ICG distribution in pregnant mice and their fetuses in the presence and the absence of valspodar. Mice were treated as described for Figure 1. Tissue emission intensity and tissue:blood ratios are presented in panels A and B, respectively. The numbers of animals were 8 and 9 for the control and valspodar-treated groups at mid-pregnancy and 6 in each of the control- and valspodar groups at late-pregnancy, respectively. Significantly different from vehicle-treated mice of the same gestational age: *$p < 0.05$; **$p < 0.01$; Mann−Whitney test.

treatment with rifampin (Figure 3D). For the most part, the results obtained following the injection of 20 mg/kg rifampin to one animal in late-pregnancy were within the ranges obtained for the animals treated with 10 mg/kg (Supporting Information). Thus, we averaged the results across all 4 animals.

As in the dams, ICG concentrated in the fetal liver. The signal in the fetal brain was lesser than in other body parts in both the absence and the presence of transporter inhibitors (Figure 4). A quantitative analysis of the effect of rifampin and valspodar on ICG distribution within late-gestation fetuses revealed increases in ICG accumulation in fetal legs (a reference region), liver, and brain following treatment with each of the transporter inhibitors (Figure 4B,D). The liver:leg and the brain:leg ratios were not affected by rifampin or valspodar (Figure 4C,E).

DISCUSSION

The transfer of ICG to fetal blood has been shown in humans to be negligible.[2,14−18] This is likely due to high binding to plasma proteins,[3−6] limited diffusion, and the absence of efficient transport mechanisms for ICG, at least in the mother-to-fetus direction. In this study we demonstrated in mice that ICG accumulates in the fetal liver and that concomitant medications that affect maternal ICG's kinetics significantly enhance fetal exposure.

Impact of Valspodar and Rifampin on Maternal ICG Distribution. The transporter inhibitors selected for this study were valspodar and rifampin. Valspodar is an established P-gp, MRP2,[24] and MDR3[25] inhibitor, whereas rifampin inhibits the

DOI: 10.1021/acs.molpharmaceut.5b00374
Mol. Pharmaceutics 2015, 12, 3351−3357

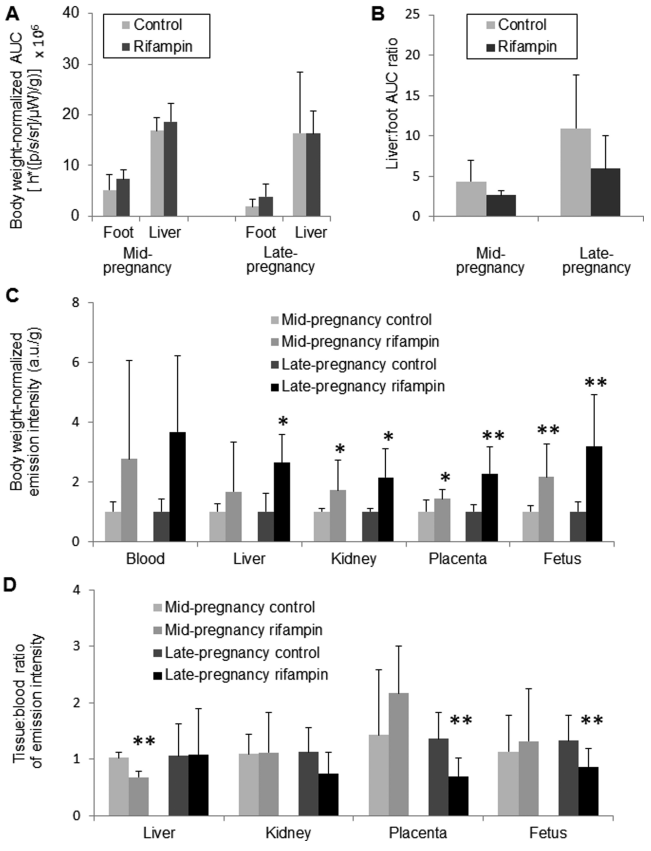

Figure 3. Rifampin increases the emission of ICG in the placenta and the fetus. Mice in mid- or late-pregnancy were treated with 20 mg/kg (n = 1, in late-pregnancy) or 10 mg/kg (all other mice) rifampin or the vehicle. Shown are $AUC_{0-30min}$ values of ICG emission intensity (A) and the respective liver:foot emission intensity ratios (B), the ex vivo tissue emission intensity values (C), and the blood-normalized tissue emission intensity (D). Data are shown as mean ± SD. The numbers of animals were 6 and 7 in the control- and rifampin-treated mid-pregnancy groups in vivo and 6 and 8 ex vivo and 4 and 4 (both in vivo and ex vivo) in the late pregnancy groups, respectively. *p < 0.05; **p < 0.01; Mann−Whitney test.

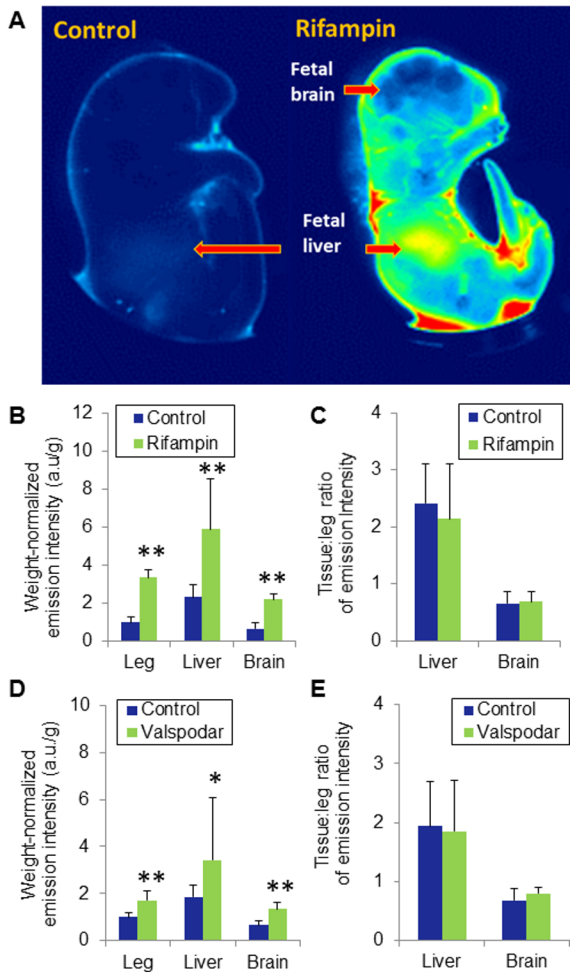

Figure 4. Rifampin and valspodar increase fetal exposure to ICG in late-pregnancy mice. ICG emission in fetuses of vehicle- and rifampin-treated dams is shown in panel A. Ex vivo analysis of emission intensity indicated that both rifampin (B, C) and valspodar (D, E) increased ICG distribution into fetal organs (B, D). However, normalization to the fetal leg signal suggested that the enhanced exposure of the fetal liver and brain is unlikely to represent transporter inhibition at barriers specific to these organs (C, E). The numbers of fetuses were 19 and 14 for control and rifampin-treated groups in the rifampin study and 18 and 17 in the control and groups in the valspodar study, respectively. *p < 0.05; **p < 0.01; Mann−Whitney test.

human OATPs 1B1, 1B3, and 1A2[26,27] and the rat Oatps 1a1 and 1a4.[28] Of note, rifampin is also a P-gp inhibitor[29] and valspodar inhibits OATP1B1,[30] OATP1B3,[31] Oatp1, and Oatp2.[31,32] Therefore, we cannot rule out inhibition of multiple transporters by each compound. This is further supported by the increased hepatic ICG concentrations when combined with rifampin. Inhibition of OATPs only would result in reduced hepatic ICG emission. Thus, it is likely that rifampin inhibited, in addition to OATPs, a hepatic efflux transport system, such as P-gp. Likewise, valspodar inhibited hepatic uptake mechanisms for ICG, as demonstrated by the reduced liver:foot ratio at late-pregnancy (Figure 1E).

Placental and Fetal ICG Distribution. P-gp[33,34] and OATPs[35,36] are important transporters at the placenta. Accordingly, both valspodar and rifampin directly inhibited to some extent placental accumulation of ICG at late pregnancy, as indicated by the lower placenta:blood ratios (Figures 2B, 3D). That is, the extent of increase in placental and fetal ICG concentration was lesser than expected based on blood ICG emission. The mechanism may be inhibition of OATPs localized at the maternal-facing apical membrane of syncytiotrophoblasts.

In previous studies in humans, in which simultaneous measurements were made in maternal and fetal blood after intravenous administration to the mother, ICG was not detectable in fetal cord blood or in umbilical vein blood collected immediately after birth. The ICG dose injected intravenously to the mothers was 0.5 mg/kg[37] or 5 mg/kg,[38] the latter many times greater than the currently recommended dose for ICG angiography.[19] Nevertheless, measurements were not conducted in fetuses or newborns themselves. Our results indicate that, as in the mother, ICG accumulates in the fetal liver, and compounds that interact with ICG may further enhance hepatic (and overall fetal) accumulation. Even ICG penetration into the fetal brain, which is very limited, was enhanced at the presence of each of the transporter inhibitors (Figure 4). It appears that these compounds did not directly inhibit fetal hepatic or blood−brain barrier transporters, which may also play a critical role in fetal protection,[39] because fetal liver:leg and brain:leg ratios remained unchanged (Figure 4).

DOI: 10.1021/acs.molpharmaceut.5b00374
Mol. Pharmaceutics 2015, 12, 3351−3357

Gestation Age-Related Differences in ICG Kinetics. This study was designed to evaluate the distribution of ICG into the fetus on gestational days 12.5 (mid-pregnancy) and 17.5 (late-pregnancy), on which the mouse placenta is a relevant model of the human placenta.[40] We chose to evaluate ICG kinetics in both stages because hepatic and placental transporter activity changes during pregnancy in humans and in mice. For example, in the mouse, the expression Abcb1a (Mdr1a; one of the murine genes encoding P-gp) decreases by 40% on gestational day 15 and is unchanged on days 7.5, 10, and 19, compared to nonpregnant controls. The expression of Abcc3 (Mrp3) decreases by 30%, 70%, and 60% on gestational days 10, 15, and 19, respectively.[40] Notably, ICG is also a marker of hepatic blood flow and hepatic transporter activity. Previously, Robson et al. did not detect differences in hepatic blood flow using ICG clearance in women at 12−14 weeks', 24−26 weeks', and 36−38 weeks' gestation as compared to 10−12 weeks after delivery.[41] In another study, ICG clearance was decreased to 70% of control nonpregnant values during labor and delivery. Our study was not aimed to compare ICG kinetic between mid- and late-pregnancy. Moreover, because experiments in mid- and late-pregnancy were conducted on different study days, the observed differences may reflect between-study-day variability in addition to gestational day effects. However, transporter inhibition overall affected the maternal and fetal ICG distribution in both stages.

Study Limitations. The power to detect potential effects of transporter inhibitors on tissue distribution of ICG was limited by small animal numbers. Yet, the impact of the concomitant drugs on the transplacental transfer of ICG was high enough to allow statistical significance of the findings. Unfortunately, we could not evaluate the placental and fetal ICG distribution in vivo due to the absence of three-dimensional and anatomical imaging that would allow identifying the placenta and the fetus with greater confidence. In addition, we did not measure the absolute ICG exposure in terms of ICG mass per maternal or fetal tissues, but rather used the emission intensity as a marker of concentration.

The tissue emission intensities were not corrected for emission from maternal blood or other body fluids (e.g., bile for liver emission) due to the tissue-dependence of the emission.[23] Hence, interpretation of these data should take into account potential under- or overestimation of the inhibitor effect on ICG emission in maternal tissues. This issue is of lesser importance for overall fetal exposure that is estimated based on emission from both fetal blood and tissue.

Some discrepancies exist between the in vivo and ex vivo imaging studies. These can be explained by the semiquantitative nature of the analyses, as described above, as well as by the fact that ex vivo imaging was conducted at a single time point, usually at least 20 min after the completion of the in vivo analysis. In addition, the in vivo images represent also emission from tissues such as skin and fat, and in vivo imaging is confounded by "surface weighting" problems (anything closer to the surface will appear brighter).[23] Nevertheless, the in vivo imaging allowed repetitive and uniform studies of systemic and hepatic ICG emission within the same subject and calculation of AUC values.[23]

■ CLINICAL TRANSLATION

In pregnant women, ICG has been used for ophthalmic angiography,[2] for estimation of hepatic function,[17,41] and for measurement of cardiac output during pregnancy,[16] labor,[14] and Caesarean surgery,[15] and it has recently been suggested as a probe for visualization of placental vessels[42] and uterine blood flow.[43] Data on ICG distribution in fetal tissues are not available, and it is currently unknown to what extent our findings translate to human pregnancy. The formation of placenta differs between mice and humans. For example, prominent chorionic villus structure develops earlier in human pregnancy (by day 21 of 270) than in the mouse (gestational day 11.5).[40] Pregnancy may also affect differently transporter expression in various tissues in mice and humans. For instance, whereas P-gp-mediated renal secretion of digoxin increased during late gestation in humans,[44] during the mouse pregnancy renal P-gp protein levels remain unaffected and mRNA expression decreases.[45,46] However, overall the trends in pregnancy regarding expression and activity of drug transporters appear to be similar in humans and mice.[39,40] Furthermore, interpretation of drug transport data across the mouse placenta after gestational day 11.5 is still relevant to the human placenta, because syncytiotrophoblasts control the exchange of nutrients, hormones, and xenobiotics between the mother and fetus in both species.

Several medications which are given to pregnant women, e.g., verapamil,[47] cyclosporine,[48] and ritonavir-containing preparations,[49,50] inhibit OATPs. Although the interactions of these medications with ICG have not been evaluated in this study, they might also potentially lead to increased ICG concentrations in mother and fetus when given with ICG.

■ CONCLUSIONS

Our findings demonstrate enhanced ICG distribution into the fetus when used concomitantly with OATP or P-gp inhibitors. The increased fetal concentrations appear to be driven by higher ICG concentrations in blood. As in the dam, ICG in the fetus accumulates in the liver and accumulation is further enhanced by administration of OATPs or P-gp inhibitors to the dam. Notably, the effects of ICG on the pharmacokinetics of concomitant medications should also be considered. Therefore, until further data are available on the safety of ICG when combined with medications that affect its hepatic handling, such combinations should be used with caution.

■ ASSOCIATED CONTENT

Supporting Information

Supporting Figure 1 depicting ICG emission intensity in maternal and fetal tissues at the presence of 10 mg/kg or 20 mg/kg rifampin. The Supporting Information is available free of charge on the ACS Publications website at DOI: 10.1021/acs.molpharmaceut.5b00374.

■ AUTHOR INFORMATION

Corresponding Author

*Institute for Drug Research, Room 613, School of Pharmacy, The Hebrew University of Jerusalem, Ein Kerem, Jerusalem, 91120, Israel. Phone: 972-2-675-8667. Fax: 972-2-675-7246. E-mail: sarae@ekmd.huji.ac.il.

Author Contributions

†A.B. and M.M. contributed equally to this work.

Notes

The authors declare no competing financial interest.

DOI: 10.1021/acs.molpharmaceut.5b00374
Mol. Pharmaceutics 2015, 12, 3351−3357

■ ACKNOWLEDGMENTS

We are grateful to Mariana Scherem for her help with the in vivo studies. The authors acknowledge the support of the European Commission FP7-PEOPLE-2011-CIG Grant No. 293800, the Israel Science Foundation (ISF) Grant No. 506/13 and internal funds. S.E. is affiliated with the David R. Bloom Centre for Pharmacy and Dr. Adolf and Klara Brettler Centre for Research in Molecular Pharmacology and Therapeutics at The Hebrew University of Jerusalem, Israel.

■ ABBREVIATIONS USED

a.u., arbitrary units; AUC, area under the concentration−time curve; FDA, Food and Drug Administration; ICG, indocyanine green; IVIS, in vivo imaging system; MDR, multidrug resistance protein; MRP, multidrug resistance associated protein; NIR, near-infrared; OATP, organic anion transporting polypeptide; [p/s/sr]/μW, [photons/second/steradian]/microwatt; P-gp, P-glycoprotein; ROI, region of interest

■ REFERENCES

(1) Caesar, J.; Shaldon, S.; Chiandussi, L.; Guevara, L.; Sherlock, S. The use of indocyanine green in the measurement of hepatic blood flow and as a test of hepatic function. *Clin. Sci.* **1961**, *21*, 43−57.

(2) Fineman, M. S.; Maguire, J. I.; Fineman, S. W.; Benson, W. E. Safety of indocyanine green angiography during pregnancy: a survey of the retina, macula, and vitreous societies. *Arch. Ophthalmol.* **2001**, *119*, 353−355.

(3) Baker, K. J. Binding of sulfobromophthalein (BSP) sodium and indocyanine green (ICG) by plasma alpha-1 lipoproteins. *Exp. Biol. Med.* **1966**, *122*, 957−63.

(4) Cherrick, G. R.; Stein, S. W.; Leevy, C. M.; Davidson, C. S. Indocyanine green: observations on its physical properties, plasma decay, and hepatic extraction. *J. Clin. Invest.* **1960**, *39*, 592−600.

(5) Kamisaka, K.; Yatsuji, Y.; Yamada, H.; Kameda, H. The binding of indocyanine green and other organic anions to serum proteins in liver diseases. *Clin. Chim. Acta* **1974**, *53*, 255−64.

(6) Yoneya, S.; Saito, T.; Komatsu, Y.; Koyama, I.; Takahashi, K.; Duvoll-Young, J. Binding properties of indocyanine green in human blood. *Invest. Ophthalmol. Visual Sci.* **1998**, *39*, 1286−1290.

(7) Hoekstra, L. T.; de Graaf, W.; Nibourg, G. A.; Heger, M.; Bennink, R. J.; Stieger, B.; van Gulik, T. M. Physiological and biochemical basis of clinical liver function tests: a review. *Ann. Surg.* **2013**, *257*, 27−36.

(8) de Graaf, W.; Häusler, S.; Heger, M.; van Ginhoven, T. M.; van Cappellen, G.; Bennink, R. J.; Kullak-Ublick, G. A.; Hesselmann, R.; van Gulik, T. M.; Stieger, B. Transporters involved in the hepatic uptake of (99m)Tc-mebrofenin and indocyanine green. *J. Hepatol.* **2011**, *54*, 738−45.

(9) Huang, L.; Vore, M. Multidrug resistance p-glycoprotein 2 is essential for the biliary excretion of indocyanine green. *Drug Metab. Dispos.* **2001**, *29*, 634−637.

(10) Portnoy, E.; Gurina, M.; Magdassi, S.; Eyal, S. Evaluation of the near infrared compound indocyanine green as a probe substrate of P-glycoprotein. *Mol. Pharmaceutics* **2012**, *9*, 3595−601.

(11) Bahmani, B.; Lytle, C. Y.; Walker, A. M.; Gupta, S.; Vullev, V. I.; Anvari, B. Effects of nanoencapsulation and PEGylation on biodistribution of indocyanine green in healthy mice: quantitative fluorescence imaging and analysis of organs. *Int. J. Nanomed.* **2013**, *8*, 1609−1620.

(12) Portnoy, E.; Nizri, E.; Golenser, J.; Shmuel, M.; Magdassi, S.; Eyal, S. Imaging the urinary pathways in mice by liposomal indocyanine green. *Nanomedicine* **2015**, *11*, 1057−1064.

(13) Yaseen, M. A.; Yu, J.; Wong, M. S.; B, A. In-vivo fluorescence imaging of mammalian organs using charge-assembled mesocapsule constructs containing indocyanine green. *Opt. Express* **2008**, *16*, 20577−20587.

(14) Lees, M. M.; Scott, D. B.; Kerr, M. G. Haemodynamic changes associated with labour. *BJOG* **1970**, *77*, 29−36.

(15) Lees, M. M.; Scott, D. B.; Slawson, K. B.; Kerr, M. G. Hemodynamic changes during Caesarean section. *BJOG* **1968**, *75*, 546−51.

(16) Lees, M. M.; Taylor, S. H.; Scott, D. B.; Kerr, M. G. A study of cardiac output at rest throughout pregnancy. *BJOG* **1967**, *74*, 319−28.

(17) Mati, J. K.; Kahuho, S. K. The measurement of indocyanine green retention in the differential diagnosis of hypertension during pregnancy. *BJOG* **1974**, *81*, 57−60.

(18) Rudolf, K.; Rudolf, H.; Töwe, J. The indocyanine green (Ujoviridin) test in patients with hyperemesis gravidarum. *Zentralbl. Gynakol.* **1982**, *104*, 748−752.

(19) Akorn, Inc. *IC-GREEN (Indocyanine Green for Injection, USP) product monograph, Revised 09/2006*; Akorn, Inc.: Buffalo Grove, IL.

(20) Eyal, S.; Hsiao, P.; Unadkat, J. D. Drug interactions at the blood-brain barrier: fact or fantasy? *Pharmacol. Ther.* **2009**, *123*, 80−104.

(21) van de Steeg, E.; Wagenaar, E.; van der Kruijssen, C. M.; Burggraaff, J. E.; de Waart, D. R.; Elferink, R. P.; Kenworthy, K. E.; Schinkel, A. H. Organic anion transporting polypeptide 1a/1b-knockout mice provide insights into hepatic handling of bilirubin, bile acids, and drugs. *J. Clin. Invest.* **2010**, *120*, 2942−52.

(22) Morrissey, K. M.; Wen, C. C.; Johns, S. J.; Zhang, L.; Huang, S. M.; Giacomini, K. M. The UCSF-FDA TransPortal: A Public Drug Transporter Database. *Clin. Pharmacol. Ther.* **2012**, *92*, 545−6.

(23) Mann, A.; Semenenko, I.; Meir, M.; Eyal, S. Molecular imaging of membrane transporters' activity in cancer: a picture is worth a thousand tubes. *AAPS J.* **2015**, *17*, 788−801.

(24) Choo, E.; Leake, B.; Wandel, C.; Imamura, H.; Wood, A.; Wilkinson, G.; Kim, R. Pharmacological inhibition of P-glycoprotein transport enhances the distribution of HIV-1 protease inhibitors into brain and testes. *Drug Metab. Dispos.* **2000**, *28*, 655−660.

(25) Smith, A. J.; van Helvoort, A.; van Meer, G.; Szabo, K.; Welker, E.; Szakacs, G.; Varadi, A.; Sarkadi, B.; Borst, P. MDR3 P-glycoprotein, a phosphatidylcholine translocase, transports several cytotoxic drugs and directly interacts with drugs as judged by interference with nucleotide trapping. *J. Biol. Chem.* **2000**, *275*, 23530−23539.

(26) Izumi, S.; Nozaki, Y.; Maeda, K.; Komori, T.; Takenaka, O.; Kusuhara, H.; Sugiyama, Y. Investigation of the impact of substrate selection on in vitro organic anion transporting polypeptide 1B1 inhibition profiles for the prediction of drug-drug interactions. *Drug Metab. Dispos.* **2015**, *43*, 235−247.

(27) Vavricka, S. R.; Van Montfoort, J.; Ha, H. R.; Meier, P. J.; Fattinger, K. Interactions of rifamycin SV and rifampicin with organic anion uptake systems of human liver. *Hepatology* **2002**, *36*, 164−172.

(28) Fattinger, K.; Cattori, V.; Hagenbuch, B.; Meier, P. J.; Stieger, B. Rifamycin SV and rifampicin exhibit differential inhibition of the hepatic rat organic anion transporting polypeptides, Oatp1 and Oatp2. *Hepatology* **2000**, *32*, 82−6.

(29) Zong, J.; Pollack, G. M. Modulation of P-glycoprotein transport activity in the mouse blood-brain barrier by rifampin. *J. Pharmacol. Exp. Ther.* **2003**, *306*, 556−562.

(30) Oostendorp, R. L.; van de Steeg, E.; van der Kruijssen, C. M.; Beijnen, J. H.; Kenworthy, K. E.; Schinkel, A. H.; Schellens, J. H. Organic anion-transporting polypeptide 1B1 mediates transport of Gimatecan and BNP1350 and can be inhibited by several classic ATP-binding cassette (ABC) B1 and/or ABCG2 inhibitors. *Drug Metab. Dispos.* **2009**, *37*, 917−23.

(31) Karlgren, M.; Vildhede, A.; Norinder, U.; Wisniewski, J. R.; Kimoto, E.; Lai, Y.; Haglund, U.; Artursson, P. Classification of inhibitors of hepatic organic anion transporting polypeptides (OATPs): influence of protein expression on drug-drug interactions. *J. Med. Chem.* **2012**, *55*, 4740−63.

(32) Cvetkovic, M.; Leake, B.; Fromm, M.; Wilkinson, G.; Kim, R. OATP and P-glycoprotein transporters mediate the cellular uptake and excretion of fexofenadine. *Drug Metab. Dispos.* **1999**, *27*, 866−871.

(33) Eyal, S.; Chung, F. S.; Muzi, M.; Link, J. M.; Mankoff, D. A.; Kaddoumi, A.; O'Sullivan, F.; Hebert, M. F.; Unadkat, J. D. Simultaneous PET imaging of P-plycoprotein inhibition in multiple

DOI: 10.1021/acs.molpharmaceut.5b00374
Mol. Pharmaceutics 2015, 12, 3351−3357

tissues in the pregnant non-human primate. *J. Nucl. Med.* **2009**, *50*, 798−806.
(34) Smit, J. W.; Huisman, M. T.; van Tellingen, O.; Wiltshire, H. R.; Schinkel, A. H. Absence or pharmacological blocking of placental P-glycoprotein profoundly increases fetal drug exposure. *J. Clin. Invest.* **1999**, *104*, 1441−7.
(35) Grube, M.; Reuther, S.; Meyer Zu Schwabedissen, H.; Köck, K.; Draber, K.; Ritter, C. A.; Fusch, C.; Jedlitschky, G.; Kroemer, H. K. Organic anion transporting polypeptide 2B1 and breast cancer resistance protein interact in the transepithelial transport of steroid sulfates in human placenta. *Drug Metab. Dispos.* **2007**, *35*, 30−35.
(36) Tertti, K.; Petsalo, A.; Niemi, M.; Ekblad, U.; Tolonen, A.; Rönnemaa, T.; Turpeinen, M.; Heikkinen, T.; Laine, K. Transfer of repaglinide in the dually perfused human placenta and the role of organic anion transporting polypeptides (OATPs). *Eur. J. Pharm. Sci.* **2011**, *44*, 181−6.
(37) Rudolf, H.; Göretzlehner, G.; Brügmann, E.; Töwe, J.; Rudolf, K. Assessment of liver function using indocyanine green (Ujoviridin) during normal pregnancy, during labor and in puerperium. *Zentralbl. Gynakol.* **1977**, *99*, 1548−1553.
(38) Probst, P.; Paumgartner, G.; Caucig, H.; Fröhlich, H.; Grabner, G. Studies on clearance and placental transfer of indocyanine green during labor. *Clin. Chim. Acta* **1970**, *29*, 157−60.
(39) Isoherranen, N.; Thummel, K. E. Drug metabolism and transport during pregnancy: how does drug disposition change during pregnancy and what are the mechanisms that cause such changes? *Drug Metab. Dispos.* **2013**, *41*, 256−62.
(40) Shuster, D. L.; Bammler, T. K.; Beyer, R. P.; Macdonald, J. W.; Tsai, J. M.; Farin, F. M.; Hebert, M. F.; Thummel, K. E.; Mao, Q. Gestational age-dependent changes in gene expression of metabolic enzymes and transporters in pregnant mice. *Drug Metab. Dispos.* **2013**, *41*, 332−42.
(41) Robson, S. C.; Mutch, E.; Boys, R. J.; Woodhouse, K. W. Apparent liver blood flow during pregnancy: a serial study using indocyanine green clearance. *BJOG* **1990**, *97*, 720−4.
(42) Harada, K.; Miwa, M.; Fukuyo, T.; Watanabe, S.; Enosawa, S.; Chiba, T. ICG fluorescence endoscope for visualization of the placental vascular network. *Minimally Invasive Ther. Allied Technol.* **2009**, *18*, 3−7.
(43) Kisu, I.; Banno, K.; Mihara, M.; Lin, L. Y.; Tsuji, K.; Yanokura, M.; Hara, H.; Araki, J.; Iida, T.; Abe, T.; Kouyama, K.; Suganuma, N.; Aoki, D. Indocyanine green fluorescence imaging for evaluation of uterine blood flow in cynomolgus macaque. *PLoS One* **2012**, *7*, e35124.
(44) Hebert, M. F.; Easterling, T. R.; Kirby, B.; Carr, D. B.; Buchanan, M. L.; Rutherford, T.; Thummel, K. E.; Fishbein, D. P.; Unadkat, J. D. Effects of pregnancy on CYP3A and P-glycoprotein activities as measured by disposition of midazolam and digoxin: a University of Washington specialized center of research study. *Clin. Pharmacol. Ther.* **2008**, *84*, 248−53.
(45) Mathias, A. A.; Maggio-Price, L.; Lai, Y.; Gupta, A.; Unadkat, J. D. Changes in pharmacokinetics of anti-HIV protease inhibitors during pregnancy: the role of CYP3A and P-glycoprotein. *J. Pharmacol. Exp. Ther.* **2006**, *316*, 1202−1209.
(46) Zhang, H.; Wu, X.; Wang, H.; Mikheev, A. M.; Mao, Q.; Unadkat, J. D. Effect of pregnancy on cytochrome P450 3a and P-glycoprotein expression and activity in the mouse: mechanisms, tissue specificity, and time course. *Mol. Pharmacol.* **2008**, *74*, 714−23.
(47) Kantola, T.; Kivistö, K. T.; Neuvonen, P. J. Erythromycin and verapamil considerably increase serum simvastatin and simvastatin acid concentrations. *Clin. Pharmacol. Ther.* **1998**, *64*, 177−82.
(48) Simonson, S. G.; Raza, A.; Martin, P. D.; Mitchell, P. D.; Jarcho, J. A.; Brown, C. D.; Windass, A. S.; Schneck, D. W. Rosuvastatin pharmacokinetics in heart transplant recipients administered an antirejection regimen including cyclosporine. *Clin. Pharmacol. Ther.* **2004**, *76*, 167−177.
(49) Busti, A. J.; Bain, A. M.; Hall, R. G.; Bedimo, R. G.; Leff, R. D.; Meek, C.; Mehvar, R. Effects of atazanavir/ritonavir or fosamprenavir/ritonavir on the pharmacokinetics of rosuvastatin. *J. Cardiovasc. Pharmacol.* **2008**, *51*, 605−10.
(50) Kiser, J. J.; Gerber, J. G.; Predhomme, J. A.; Wolfe, P.; Flynn, D. M.; Hoody, D. W. Drug/Drug interaction between lopinavir/ritonavir and rosuvastatin in healthy volunteers. *JAIDS, J. Acquired Immune Defic. Syndr.* **2008**, *47*, 570−8.

DOI: 10.1021/acs.molpharmaceut.5b00374
Mol. Pharmaceutics 2015, 12, 3351−3357